Validation and Bias Correction of Forecast Reference Evapotranspiration for Agricultural Applications in Nevada

Daniel J. McEvoy[1]; Shawn Roj[2]; Christian Dunkerly[3]; David McGraw[4]; Justin L. Huntington[5]; Mike T. Hobbins[6]; and Thomas Ott[7]

Abstract: Accurate estimates of reference evapotranspiration (ET_0) are critical for estimating actual crop evapotranspiration and agricultural water use. This study uses observations from the Nevada Integrated Climate and Evapotranspiration Network (NICE Net) to validate forecasts of ET_0 and its driving variables from the National Weather Service's National Digital Forecast Database (NDFD). Daily NDFD ET_0 at lead times of 1 to 6 days were compared against 18 NICE Net stations. Correlations between NDFD and observations generally ranged between 0.4 and 0.9, with lower correlations at longer leads and a notable drop in skill during July and August. Systematic arid biases (high bias for temperatures and low bias for humidity) were found in NDFD with a strong warm minimum temperature bias and low vapor pressure bias most prominent during the growing season. Some of the largest relative biases were found in wind speed, although they were systematic and varied greatly by location. A case study revealed that NDFD consistently underestimates the variability found in observed minimum temperature, solar radiation, wind speed, and ET_0. Cloudy days during summer were not well represented in the NDFD estimated solar radiation, which had a cascading impact on temperature, vapor pressure, and ET_0 estimates. A monthly ratio-based bias-correction was applied to NDFD ET_0, which reduced the root-mean squared error by 5%–30% for most locations. Bias-corrected ET_0 forecasts from NDFD or other forecast systems show potential as a guide to develop weekly irrigation schedules for agricultural producers, with the ultimate goal of reducing applications of excess irrigation water. **DOI: 10.1061/(ASCE)WR.1943-5452.0001595.**

Introduction

The 2017 Census of Agriculture stated that the total area of irrigated land in the US is approximately 23 million ha (58 million acres) (NASS 2019); the associated water rights are worth over $200 billion (Allen et al. 2015). Accurate operational estimates of agricultural evapotranspiration (*ET*) are therefore a national necessity. Further, the western US faces increasing pressure to conserve water and reduce consumptive water use in the face of prolonged drought and a changing climate (Blumler 2018). Because irrigated agriculture consumes most permitted water rights in the western US (Dieter et al. 2018), the biggest opportunity to save water is through reducing consumptive uses of irrigation, particularly through the use of new technologies such as in situ field monitoring, high-resolution weather forecasts, and precision irrigation systems (Allmaras et al. 2018).

Accurately measuring *ET* to estimate consumptive use can be difficult and expensive, so most agricultural regions lack actual *ET* measurements. To overcome this limitation, reference evapotranspiration (ET_0) is commonly used to estimate actual *ET* in support of irrigation scheduling (Hobbins and Huntington 2016). A form of evaporative demand, ET_0 is parameterized to represent the *ET* from a well-watered reference crop (Allen et al. 2005), and it is generated from local weather data observations of temperature, humidity, wind speed, and solar radiation. The generated values are then used as an evaporative index to permit decision makers such as engineers, hydrologists, and water managers to predict *ET* for agricultural areas that are well-watered (Allen et al. 2005). For agricultural applications, accurate forecasts of *ET* can help support and complement conservation efforts by identifying optimal times and days for irrigation, optimizing application amounts, and providing for data-informed deficit irrigation.

Global weather forecast models provide the variables needed to compute ET_0, but at too coarse a spatial resolution for agricultural applications, necessitating downscaling (e.g., Tian and Martinez 2014). Gridded high-resolution (5 km) forecasts of meteorological variables from the National Weather Service (NWS 2018) were first produced in 2003 with the development of the National Digital Forecast Database (NDFD) (Glahn and Ruth 2003); the forecast reference evapotranspiration (FRET) was added as an operational

[1]Associate Professor, Division of Atmospheric Sciences, Desert Research Institute, 2215 Raggio Parkway, Reno, NV 89512; Western Regional Climate Center, Reno, NV 89512 (corresponding author). ORCID: https://orcid.org/0000-0003-3800-718X. Email: mcevoyd@dri.edu

[2]Researcher, Staff, Contract, Scripps Institute of Oceanography, 8622 Kennel Way, La Jolla, CA 92037. ORCID: https://orcid.org/0000-0003-0515-0270. Email: shawnroj78@gmail.com

[3]Research Scientist, Division of Hydrologic Sciences, Desert Research Institute, 2215 Raggio Parkway, Reno, NV 89512. Email: christian.dunkerly@dri.edu

[4]Assistant Research Scientist, Division of Hydrologic Sciences, Desert Research Institute, 2215 Raggio Parkway, Reno, NV 89512. Email: david.s.mcgraw@gmail.com

[5]Professor, Division of Hydrologic Sciences, Desert Research Institute, 2215 Raggio Parkway, Reno, NV 89512; Western Regional Climate Center, Reno, NV 89512. Email: justin.huntington@dri.edu

[6]Research Hydrologist, Cooperative Institute for Research in Environmental Sciences, Univ. of Colorado Boulder, 216 UCB, Boulder, CO 80309; National Oceanic and Atmospheric Administration/Physical Sciences Laboratory, 325 Broadway, Boulder, CO 80305. ORCID: https://orcid.org/0000-0001-5540-8466. Email: mike.hobbins@noaa.gov

[7]Assistant Research Scientist, Division of Hydrologic Sciences, Desert Research Institute, 2215 Raggio Parkway, Reno, NV 89512. Email: thomas.ott@dri.edu

Note. This manuscript was submitted on December 12, 2021; approved on May 22, 2022; published online on August 29, 2022. Discussion period open until January 29, 2023; separate discussions must be submitted for individual papers. This paper is part of the ***Journal of Water Resources Planning and Management***, © ASCE, ISSN 0733-9496.

output variable in 2016. However, thus far, studies validating FRET have been limited to California (Krone-Davis et al. 2012; Hamouda et al. 2022) and New Mexico (Engle et al. 2019) and have focused on annual or seasonal comparison with observations, and these studies have yet to assess the individual drivers used to compute FRET.

Weather forecasts in general do not assimilate agricultural land information into their modeling systems. Irrigation increases *ET* and affects land surface-atmospheric feedbacks (Ozdogan and Rodell 2010). Even in highly advective arid environments, land surface-atmospheric feedbacks and near-surface boundary layer conditioning within irrigated areas has been well-documented (Allen et al. 1983; Temesgen et al. 1999; Szilagyi and Schepers 2014; Huntington et al. 2015, 2018). The near-surface (i.e., 2-m) air temperature is lower, humidity is higher, and wind speeds are lower in irrigated areas than in surrounding arid landscapes. These differences are typical when comparing reanalysis data with agricultural weather station–derived variables and ET_0 (Lewis et al. 2014; Blankenau 2017).

They also follow well-known complementary theory, where an increase in actual *ET* results in a decrease in evaporative demand (i.e., ET_0) (Brutsaert and Parlange 1998; Hobbins et al. 2004; Hobbins and Huntington 2016). Abatzoglou (2011) also noted a positive bias in ET_0 derived from a reanalysis hybrid of the North American Land Data Assimilation System (NLDAS) (Mitchell et al. 2004) and the Parameter Regression on Independent Slopes Model (PRISM) (Daly et al. 2002) when compared with ET_0 computed from data collected from US Bureau of Reclamation's AgriMET stations in the US Pacific Northwest. Despite this common knowledge within the *ET* community, researchers and practitioners routinely and erroneously apply reference *ET* equations to estimate well-watered reference and potential crop *ET* using ambient weather data representative of water-limited arid conditions, rather than using weather data representative of local agricultural conditions. This practice can lead to excess irrigation and wasted water supply.

A bias-corrected FRET product has the potential to reduce avoidable nonbeneficial consumptive uses by informing irrigators when to vary the application rate of conventional high-pressure or newer low-energy precision application (LEPA) center-pivot irrigation systems, when to turn the irrigation systems off completely on days when ET_0 is forecast to be low or to continue application on days where ET_0 is forecast to be high (M. P. Plaskett, personal communication, 2019). Current practice in Nevada is to run conventional irrigation systems at constant speeds and pumping rates throughout the day. Therefore, integrating the 7-day FRET into irrigation management and operations and implementing LEPA systems has the greatest potential to reduce application rates and nonbeneficial consumptive uses beyond typical reported values of 20% to 30% (Lyle and Bordovsky 1983; Fipps and New 1990; Rajan et al. 2015).

In this study, we examine the forecast skill of FRET and NDFD compared against agricultural weather station observations in Nevada. We build upon existing studies that have assessed FRET by (1) using the individual NDFD ET_0 drivers to determine which variables are contributing most to forecast errors, (2) performing comparisons monthly (as opposed to seasonal or annual), and (3) providing a method to apply a bias-correction to ET_0 forecasts. First, the collection of ET_0 observations and data QC is described, followed by a description of NDFD and FRET. Then, we describe the results of the skill analysis over Nevada and provide a station-based case study. Finally, we show a comparison of the forecast errors before and after bias correction.

Data and Methods

Reference Evapotranspiration Observations and Quality Control

Daily weather observations were gathered from the Nevada Integrated Climate and Evapotranspiration Network (NICE Net, Desert Research Institute, n.d.-a) run by the Desert Research Institute (Fig. 1). The network consists of 18 agricultural weather stations located throughout Nevada and one station located in eastern California [Fig. 1(a)]. NICE Net stations were installed beginning in 2010 to collect weather data representative of agricultural areas in Nevada and enable a more accurate estimation of agricultural water use across the state. Stations are typically located on the edges of irrigated fields [Figs. 1(b and c)] to capture the modified near-surface boundary layer weather conditions associated with irrigated lands in arid regions. NICE Net stations collect measurements of solar radiation, air temperature at 2 m, relative humidity at 2 m, wind speed at 3 m, and precipitation, barometric pressure, and soil temperature and soil moisture at multiple depths. Daily records were downloaded for the period of record at each station. Station metadata can be found in Table 1.

Weather station data were subject to quality assurance and quality control (QAQC) following QAQC recommendations and guidelines of Allen (1996), Allen et al. (2011), and ASCE (Allen et al. 2005), which are specific to agricultural weather data. Weather data were visualized and QAQCed using open-source Python software developed by DRI (pyWeatherQAQC, Desert Research Institute, n.d.-b).

Corrections for omissions of agricultural weather data are common and necessary prior to computing ET_0 (Allen 1996; Allen et al. 2005, 2011). As a specific example, the pyranometer recording solar radiation data may experience frequent accumulations of debris on the lens, or it may experience voltage spikes, sensor drift, or local environmental obstructions (Allen 2008). The ASCE equation requires wind speeds for a 2-m height, so wind speeds measured at a 3-m height were logarithmically transformed following guidelines of Allen et al. (2005). Details of QAQC procedures and recommendations for best results are found within the code documentation (Desert Research Institute, n.d.-b).

After completion of weather data QAQC, meteorological variables were used to compute ET_0 using the ASCE standardized Penman-Monteith (ASCE-PM) reference *ET* equation (Allen et al. 2005) for a short-grass reference crop using open-source Python software developed by DRI called the ASCE Standardized Reference Evapotranspiration Script version 0.3.10 (Desert Research Institute, n.d.-b), and is defined as follows:

$$ET_0 = \frac{0.480\Delta(R_n - G) + \gamma \frac{C_n}{T+273} u_2 (e_s - e_a)}{\Delta + \gamma(1 + C_d u_2)} \quad (1)$$

where T = daily mean temperature at 2-m height (°C); u_2 = daily mean wind speed at 2-m height ($\mathrm{m\,s^{-1}}$); R_n = daily average net radiation ($\mathrm{MJ\,m^{-2}\,day^{-1}}$); G = soil heat flux density ($\mathrm{MJ\,m^{-2}\,day^{-1}}$); e_s = daily mean saturation vapor pressure at 2-m height (kPa); e_a = daily mean actual vapor pressure at 2-m height (kPa); Δ = slope of the saturation vapor pressure-temperature curve ($\mathrm{kPa\,°C^{-1}}$); γ = psychrometric constant ($\mathrm{kPa\,°C^{-1}}$); C_n = 900 K mms^3 Mg^{-1} day^{-1} for a short-grass reference; and C_d = $0.34\,\mathrm{m\,s^{-1}}$ for a short-grass reference.

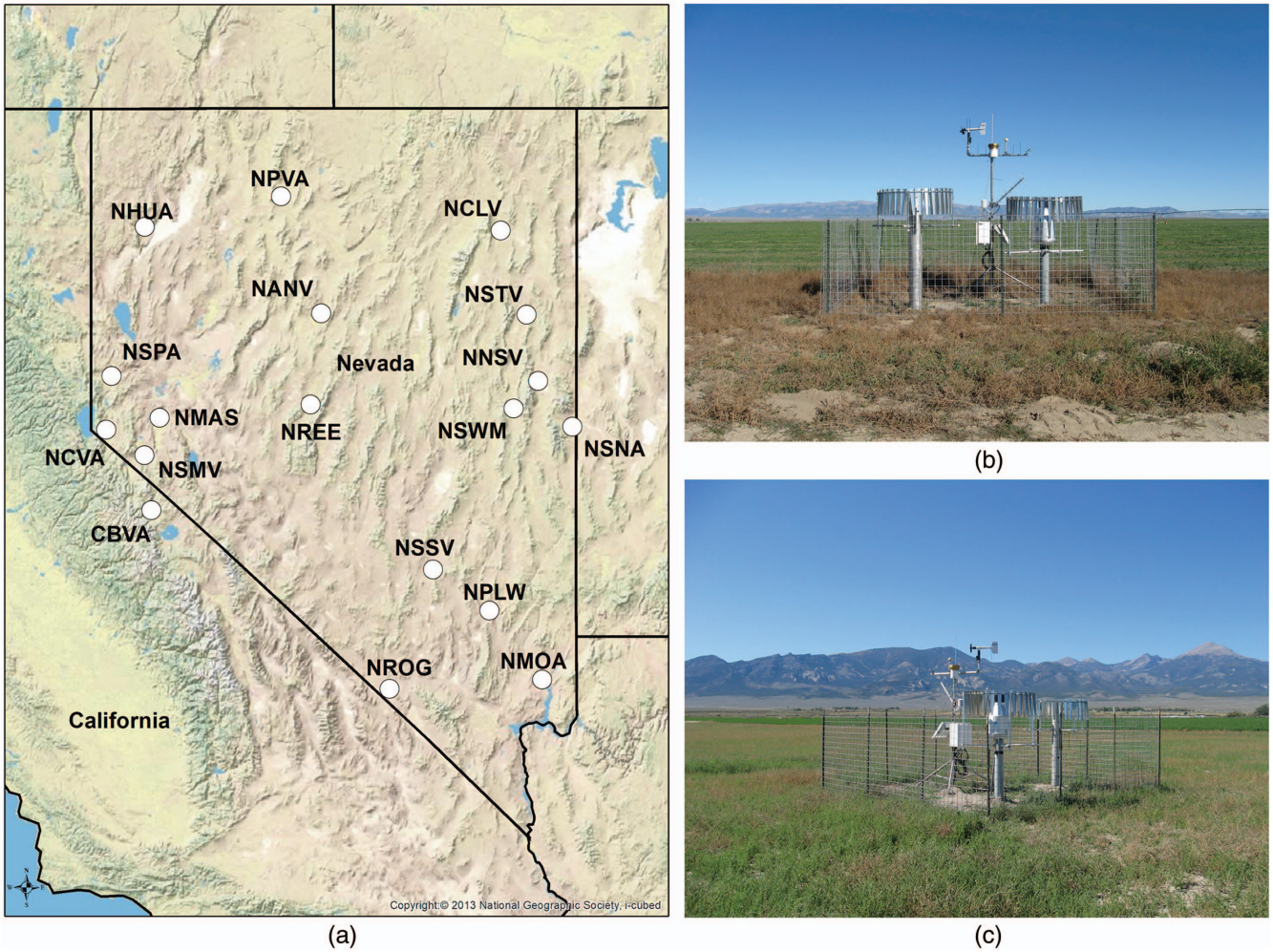

Fig. 1. (Color) (a) Location of NICE Net stations throughout Nevada and one station in eastern California; (b) Clover Valley (NSNA); and (c) Snake Valley (NCVL). Full names for the four-letter station abbreviations can be found in Table 1. Photographs from (b) Clover Valley (NCLV); and (c) Snake Valley (NSNA) were taken by Greg McCurdy (Western Regional Climate Center) and used with permission. The map was created using ArcGIS® software by Esri. ArcGIS and ArcMap are the intellectual property of Esri and are used herein under license. Copyright © Esri. All rights reserved.

Table 1. NICE Net station metadata

Station name	Station ID	Elevation (m)	Station start date
Moapa Valley	NMOA	399	February 2010
Mason WMA	NMAS	1,319	April 2010
Truckee Meadows	NSPA	1,338	May 2010
Pahranagat NWR	NPWL	983	July 2010
Carson Valley	NCVA	1,426	August 2010
Smith Valley	NSMV	1,489	August 2010
Snake Valley	NSNA	1,579	August 2010
Rogers Spring	NROG	689	September 2010
Paradise Valley	NPVA	1,341	November 2010
Sand Spring Valley	NSSV	1,466	December 2010
Steptoe Valley North	NSTV	1,785	March 2011
Steptoe Valley WMA	NSWM	1,966	March 2011
Antelope Valley	NANV	1,485	June 2011
North Spring Valley	NSPA	1,338	June 2011
Clover Valley	NCLV	1,721	September 2011
Bridgeport Valley	CBVA	1,980	July 2012
Hualapai Flat	NHUA	1,236	October 2012
Reese River Valley	NREE	1,847	May 2014

Reference ET from the National Digital Forecast Database

In 2003, the NWS began producing the NDFD (Glahn and Ruth 2003) to supplement the text-only forecasts previously available. NDFD provides continuous spatial grids across Contiguous United States (CONUS) that are mosaicked together from individual NWS Weather Forecast Offices at high resolution (5 km) with forecasts updated hourly and issued for lead times of 1–7 days. For applications such as forecasting ET_0 for agricultural water-use estimates, the high spatial resolution of the NDFD is beneficial and eliminates the need to downscale. In 2016, the NWS began producing an operational FRET) (Hobbins 2010), computed from NDFD elements and based on ET_0. The main issue with conducting a skill analysis of FRET is its short period of record (shorter than 5 years) and consequent small sample size. Most NICE Net stations have 8–10 years of data to compare against. Another limitation of using just FRET for a skill analysis is that biases and forecast errors cannot be attributed to the individual drivers of ET_0. We therefore decided to compute ET_0 offline based on NDFD elements to provide

a more robust skill analysis and development of bias-correction factors, and to examine the skill and biases of the NDFD drivers of ET_0. A comparison of FRET with the ET_0 computed in this study from NDFD variables is presented in Fig. 2 and shows strong relationships between the two. For the main study results, we show ET_0 computed offline using NDFD elements and show the FRET results in Appendix I.

From the NDFD archive (Desert Research Institute, n.d.-b), we used daily maximum temperature (T_{max}), daily minimum temperature (T_{min}), wind speed at 10 m, percent sky cover, and vapor pressure extracted from the grid point nearest to each observing station. Forecast lead times of 1–6 days were evaluated. Calculations of ET_0 were done in the same way as for observations, with the following exception: NDFD does not provide incoming shortwave radiation (R_{in}), so we had to estimate it from sky cover first. We followed the methods of Hobbins (2010) to estimate R_{in} to replicate the methods used in FRET calculations as follows:

$$R_{in} = R_{toa}\left(1 - a_{sa}\frac{CC_{daily}}{100}\right) \quad (2)$$

where R_{toa} = extraterrestrial shortwave radiation estimated based on Walter et al. (2000); a_{sa} =calibrated constant (0.71); and CC_{daily} = mean cloud cover (%) during daylight hours estimated from Brutsaert (2013).

Skill Analysis

Forecasts of NDFD ET_0 and the drivers were compared against observations to assess skill of the forecasts. Skill was assessed at leads 1–6 days and for each month of the year. Samples for skill analysis were grouped by using all days in each month for the period of record, which provided sample sizes of about 150–250 data points per month at each location. The following three statistical measures were used to gauge the skill of NDFD forecasts: the correlation coefficient (R) based on the Pearson correlation; root-mean square error (RMSE); and bias. Bias was computed as the difference (NDFD − Observations) for T_{max} and T_{min} and as the ratio (NDFD/Observations) for all other variables.

Bias Correction of NDFD ET_0 to Observed ET_0

We show how a bias-correction approach can be applied to NDFD ET_0 forecasts. We did not bias-correct the individual drivers used to compute ET_0; just the resultant ET_0 values were bias-corrected. Bias ratios computed for each month and lead time were applied to NDFD ET_0 forecasts at the daily time step. This method has been previously applied to bias-correct historical gridded weather data and gridded climate projections (Huntington et al. 2016, 2018). Forecasts and observations were pooled by month using the full period of record at each station point, and a mean $ET_0(\overline{ET_0})$ was computed for

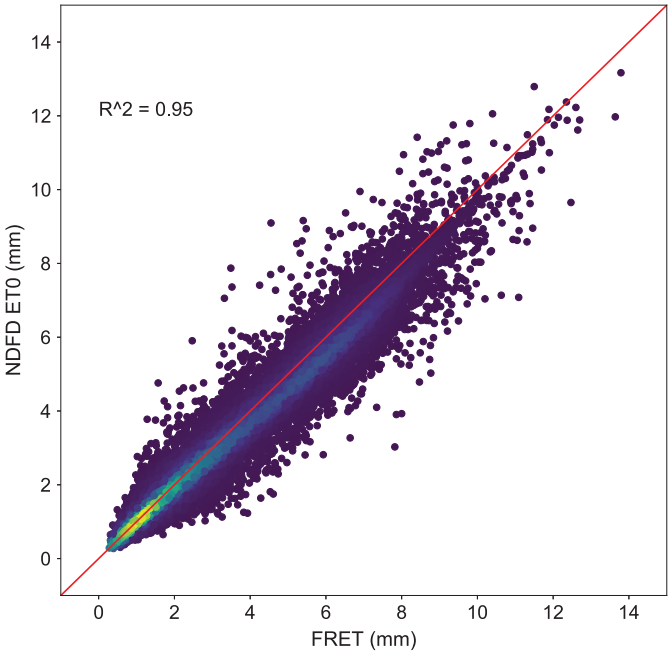

Fig. 2. (Color) Comparison of FRET and ET_0 computed from NDFD drivers. Data are from all points at all NICE Net stations using the complete period of record common to both FRET and NDFD for each location. Lead 1-day forecasts are shown. Shading indicates point density, with brighter colors (yellows) showing higher density and darker colors (blues) showing lower density.

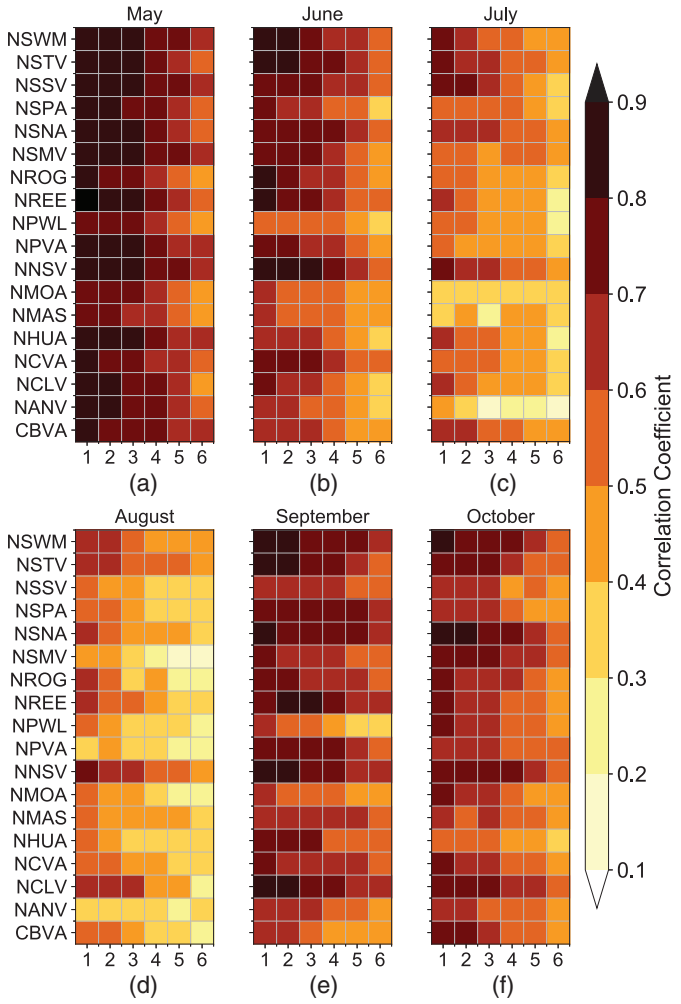

Fig. 3. (Color) Correlation coefficient R between NDFD and NICE Net ET_0 in (a) May; (b) June; (c) July; (d) August; (e) September; and (f) October. Vertical axes show the station abbreviations, and horizontal axis shows lead time in days.

each. The bias ratio (BR) for each month was then computed as follows:

$$BR = \frac{(\overline{ET_0})_{\text{NDFD}}}{(\overline{ET_0})_{\text{Observed}}} \tag{3}$$

For example, at Carson Valley (NCVA in Table 1) in June, there were at total of 235 observations (2010–2020); for each NDFD lead time, the $(\overline{ET_0})$ was computed over those 235 data points and divided by the station $(\overline{ET_0})$ for June. The bias-corrected data (ET_{0BC}) for June would be obtained by dividing the NDFD daily forecasts ($ET_{0\text{NDFD}}$) by the monthly BR

$$ET_{0BC} = \frac{ET_{0\text{NDFD}}}{BR} \tag{4}$$

The RMSE for the original forecasts were then compared with the RMSE of the bias-corrected forecasts to examine improvements in the forecasted ET_0 quantities.

Results

Growing Season Forecast Skill

The correlation between NDFD and observed ET_0 for each month (May–October) and lead time (1–6 days) is shown in Fig. 3. As expected, we found a general pattern of correlation decreasing at longer lead times. Forecasts in the month of May were the most skillful of all growing season months with R values of 0.7–0.9 during the first 4 days and a notable drop in skill for Days 5 and 6. The summer months, particularly July and August, showed a large drop in forecast skill at all lead times with R values rarely exceeding 0.7 and often in the 0.4–0.6 range even at a lead of 1 day. In September and October, skill improved again. The lower skill during July and August is concerning for agricultural applications given that climatologically, ET_0 reaches a peak during these months and irrigation rates are highest. Results showing FRET compared with observations can be found in Appendix I.

To examine possible sources of the lower correlations during summer, we used July as an example and plotted the correlations for ET_0 along with all the drivers in Fig. 4. Overall, T_{max}, solar radiation, and vapor pressure consistently had the strongest

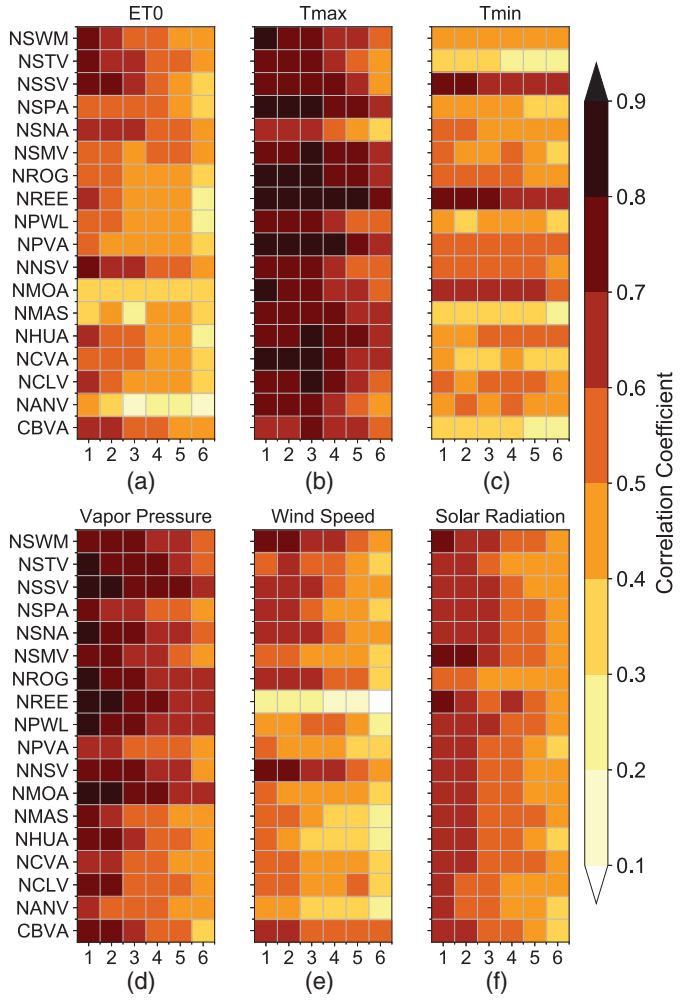

Fig. 4. (Color) Correlation coefficient R between NDFD and NICE Net (a) ET_0; (b) T_{max}; (c) T_{min}; (d) vapor pressure; (e) wind speed; and (f) solar radiation in July. Vertical axes show the station abbreviations, and horizontal axis shows lead time in days. Panel (a) is repeated from Fig. 3(c).

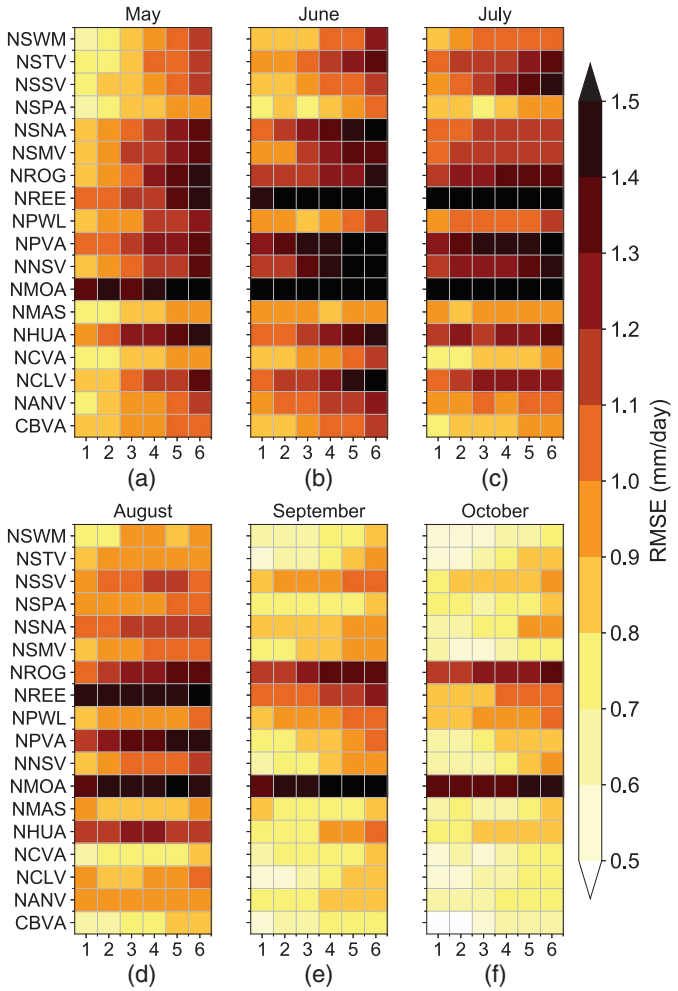

Fig. 5. (Color) RMSE between NDFD and NICE Net ET_0 in (a) May; (b) June; (c) July; (d) August; (e) September; and (f) October. Vertical axes show the station abbreviations, and horizontal axis shows lead time in days.

correlations, whereas T_{min} and wind speed had the lowest correlations. This result shows that T_{min} and wind speed were likely the main contributors to the degraded ET_0 correlations.

Fig. 5 shows the NDFD ET_0 RMSE for each month (May–October) and lead time (1–6 days). RMSE generally increased with lead time, although for some stations, RMSE remained steady over all leads or even decreased. Like the correlation analysis, the RMSE was overall greatest during the summer months. For summer, when absolute values of ET_0 were the highest, RMSE ranged from 0.65 to 1.96 mm/day. At some stations, high RMSE was found during all months and lead times, including Moapa Valley (NMOA), Reese River Valley (NREE), and Rogers Spring (NROG). Results showing FRET RMSE can be found in Appendix I.

Maximum and minimum temperature biases for each month (and growing season mean) at a lead of 1 day are shown in Figs. 6(a and b). Because monthly bias patterns were similar at all lead times and indicate systematic bias in NDFD, we chose to focus on 1-day leads, which are likely the most applicable for agricultural applications. We found a distinct seasonal pattern in bias for both T_{max} and T_{min}. For T_{min}, biases ranged from −0.53°C to +4.62°C, but were mostly positive (warm) with consistently larger values found during the growing season; for T_{max}, biases ranged from −1.90°C to +1.83°C, with negative (cool) biases often found in October–April and positive (warm) biases during May–September. Warm T_{min} biases during the growing season are due to NDFD not accounting for the well-watered and vegetated land-surface conditions at station locations, which leads to lower overnight temperatures than the surrounding arid landscapes of Nevada. Similarly, daytime high temperatures (T_{max}) tend to be higher in arid landscapes than in irrigated areas. Scale mismatches between station and 5-km grid values will also inherently lead to gridded data biases that do not capture microclimates.

Bias ratios for vapor pressure, wind speed, solar radiation, and ET_0 for each month (and growing season mean) at a 1-day lead are shown in Figs. 6(c–f). Starting with vapor pressure [Fig. 6(c)], we found consistently low NDFD bias during the growing season. Some larger vapor pressure bias ratios were found to be less than 0.75 (25%); however, smaller biases of 0.9–1.0 (<10%) were more common. The low growing-season biases in NDFD reflect the general arid bias with lower humidity relative to observations. Wind speed biases [Fig. 6(d)] were variable, but NDFD wind speed

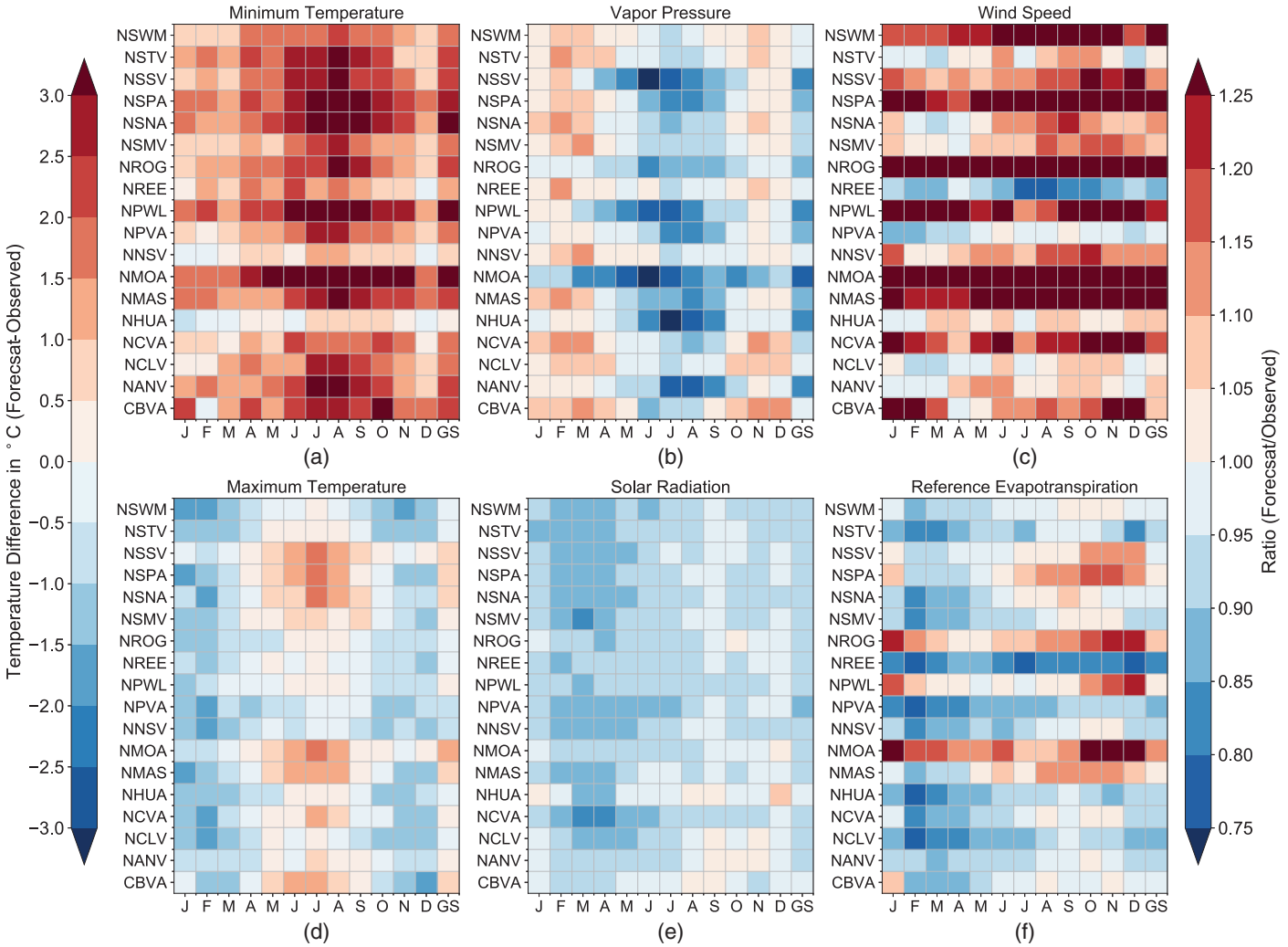

Fig. 6. (Color) NDFD biases for the lead 1-day forecasts for (a) minimum temperature; (b) maximum temperature; (c) vapor pressure; (d) wind speed; (e) solar radiation; and (f) ET_0. Horizontal axes show the calendar months (January–December) from left to right, with the growing season (GS) (May–October) average on the far right. Vertical axes show the station abbreviations.

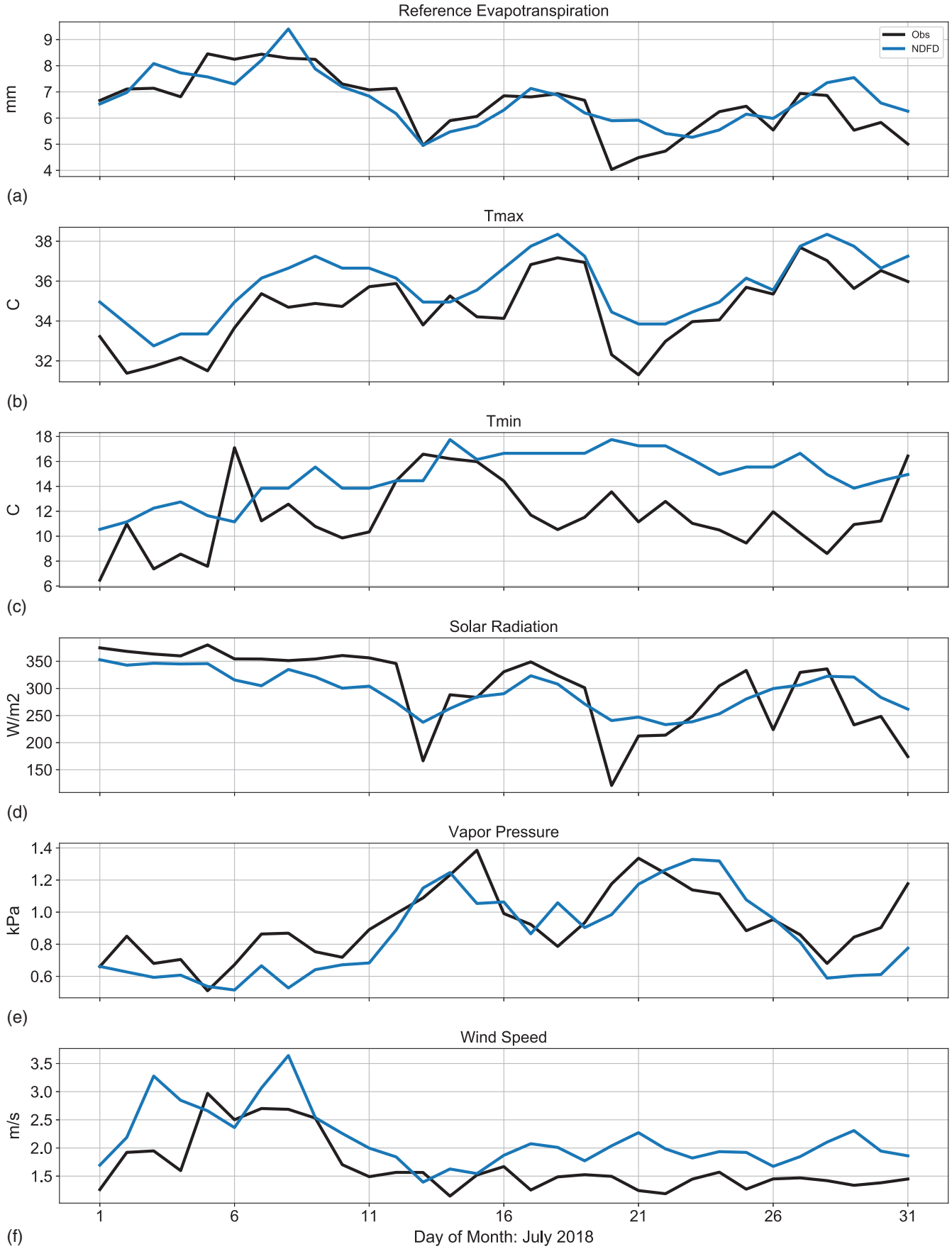

Fig. 7. (Color) Daily time series for July 2018 at NSMV (Obs) and nearest NDFD grid point for (a) ET_0; (b) vapor pressure; (c) T_{max}; (d) T_{min}; (e) wind speed; and (f) solar radiation. NDFD forecasts shown are for a 1-day lead time.

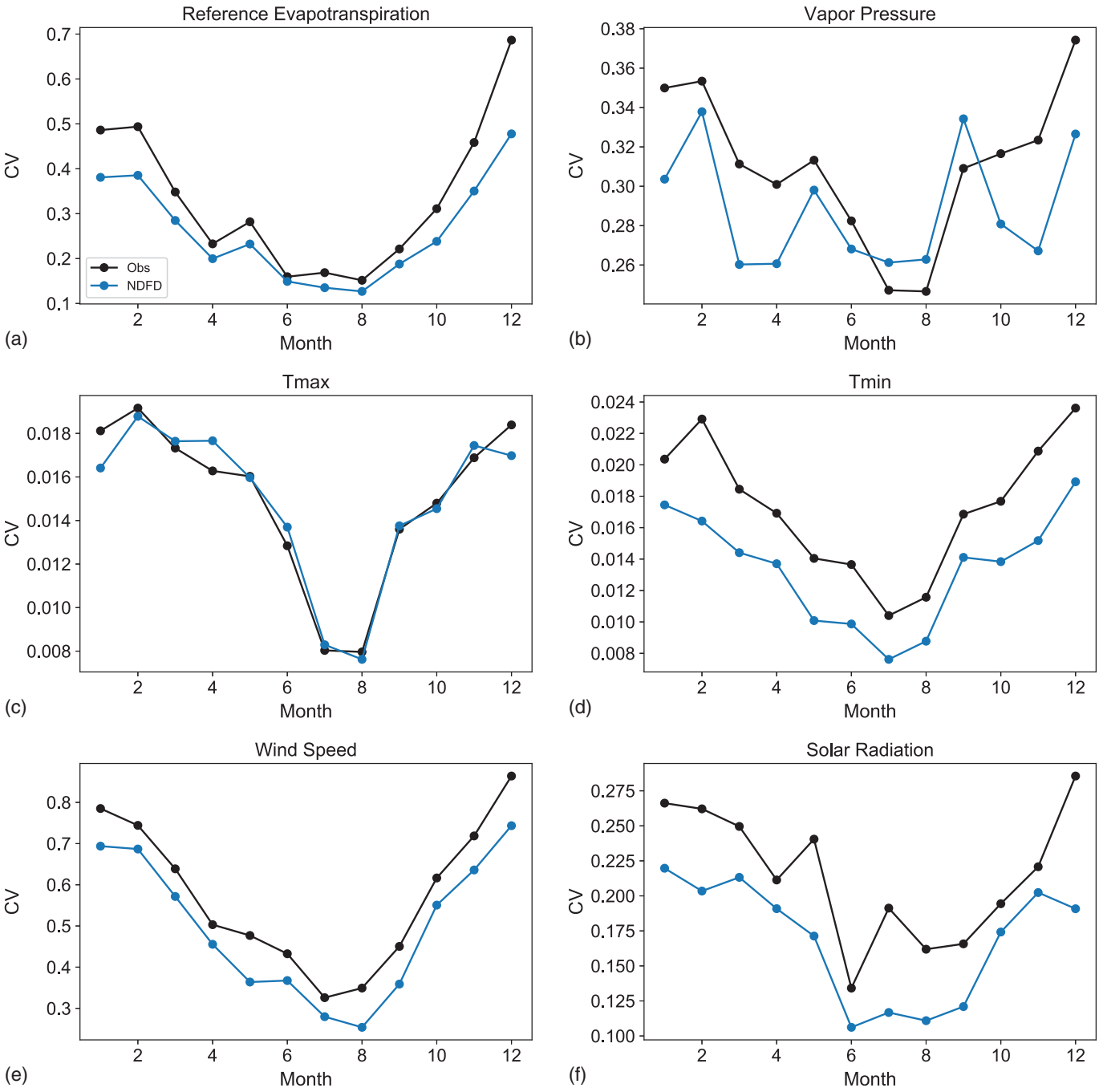

Fig. 8. (Color) Monthly (daily values averaged to the month) COV at the Smith Valley NICE Net (NSMV) (marked Obs) and nearest NDFD grid point for (a) ET_0; (b) vapor pressure; (c) T_{max}; (d) T_{min}; (e) wind speed; and (f) solar radiation. NDFD forecasts shown are for a 1-day lead time.

was higher than observations for the most part. At several locations, we found wind speed bias ratios to consistently exceed 1.25 during all months. At other locations, wind speed biases were far more reasonable, remaining within ±10% of observations.

Solar radiation [Fig. 6(e)] had the most consistent magnitude of biases when considering variations across all stations; biases were generally low, with a notably larger bias during the spring months. ET_0 biases [Fig. 6(f)] (FRET results are given in Appendix I) were also quite variable but often fell within ±10% of observations during the growing season. Next, we present a case study for an individual station to help understand how each driver contributes to NDFD ET_0 biases and errors.

Smith Valley, Nevada, Case Study

The Smith Valley NICE Net station (NSMV) is used next as a case study to examine contributions of forecast skill from individual drivers. A daily time series from July 2018 at NSMV is shown in Fig. 7 with the lead 1-day NDFD forecast overlaid. At the monthly scale, we found good agreement between the ET_0 totals from observations (202 mm) and NDFD (207 mm). Although this

is encouraging, it is the daily variations that will be most important to producers for irrigation scheduling. In general, observed ET_0 variability seemed to be captured well, with an exception being July 20–22. A light precipitation event occurred on July 20 with 3.3 mm of rainfall observed. During this period, the observed ET_0 declined to a minimum of 4.0 mm/day on July 20, whereas NDFD always exceeded 5.4 mm/day and showed no pronounced drop off. NDFD T_{max} declined but not as sharply as observed, whereas NDFD T_{min} showed a steady high bias.

Observed T_{min} variations earlier in the month were not well captured by NDFD. There was a large dip in observed solar radiation on July 20 (121 W/m^2) due to clouds that NDFD did not capture (a similar situation occurred earlier in the month), which coincides with the ET_0 minimum. Even if the sensitivity of ET_0 to solar radiation is low, cloudy days not being well resolved in NDFD will impact other variables such as T_{max}, T_{min}, and vapor pressure, ultimately contributing to a less accurate forecast for that day.

The coefficient of variation (COV) was computed by month (daily values averaged to the month) for ET_0 and each driver and is shown in Fig. 8 for NSMV. We found that NDFD was able to capture the seasonal pattern of lowest ET_0 variability in the summer months and highest during the winter, with NDFD consistently having less variability than observations throughout the entire year [Fig. 8(a)]. Of the five drivers of ET_0, the closest match was for T_{max}, with a difference within ±0%. NDFD T_{min} also followed the observed seasonal COV cycle but was consistently much lower (20%–40%) than observed. Wind speed and solar radiation from NDFD also consistently varied less than observed values. The underprediction of T_{min}, wind speed, and solar radiation COV is one factor in the reduction of forecast skill from NDFD. Results may vary at other sites (for example, at NMOA, wind speed is actually overpredicted) (Appendix II), but T_{min}, wind speed, and solar radiation consistently drive the reductions in forecast skill.

Forecast Skill Improvements with Bias Correction

Bias ratios computed for ET_0 were applied to the NDFD ET_0, and RMSE was recalculated using the bias-corrected results. Fig. 9 shows the change (%) in RMSE after the bias correction was applied (results using FRET are given in Appendix I). Decreases in RMSE were found at most locations with 5%–30% reductions in error common. Reese River Valley, Nevada (NREE), consistently had reductions in RMSE of >30% at all lead times for June–August with a 48%–50% reduction at leads of 1–3 days in June. Minor increases in error were found in some locations; these changes were negligible, with a maximum increase in RMSE of 0.73%.

Results presented in Fig. 9 show RMSE for the period of record. This does not ensure that for a real-time forecast application every single bias-corrected value will improve. Some forecasts will improve, and others will get worse, but on average there should be improvements. Also, real-time forecasted values will be independent of the values used to compute the historical bias ratios shown here, which could slightly reduce the skill shown in this paper. These results suggest that, overall, a real-time application of a monthly bias-correction ratio to NDFD ET_0 forecasts could improve estimates of ET_0 quantities needed for accurate irrigation scheduling and water conservation.

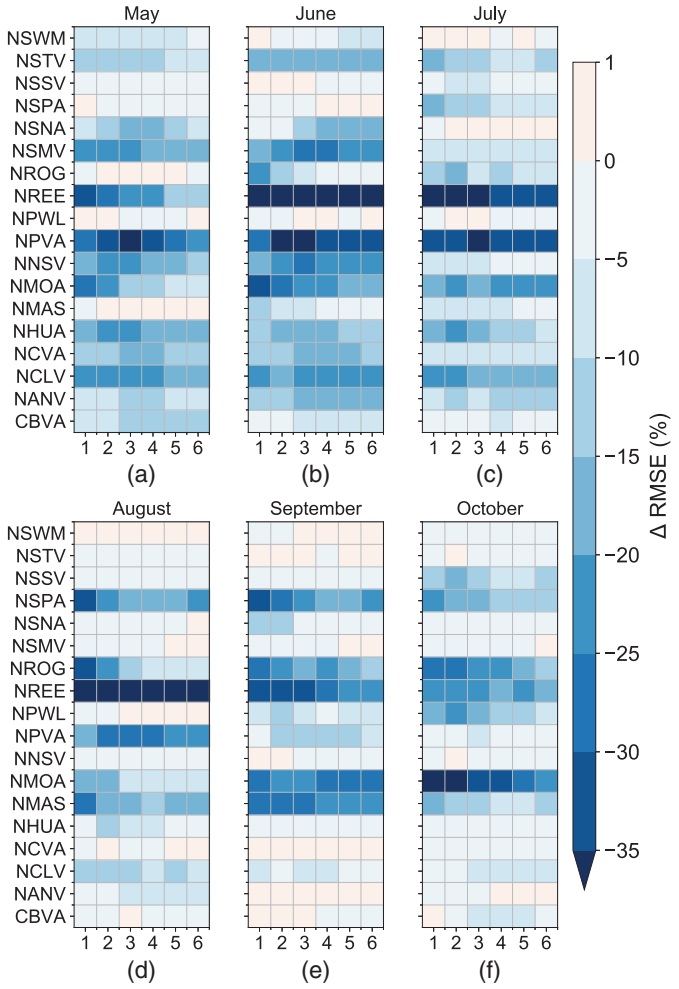

Fig. 9. (Color) Percent change in NDFD ET_0 RMSE at all lead times for (a) May; (b) June; (c) July; (d) August; (e) September; and (f) October. Percent change is calculated as [(bias corrected − uncorrected)/uncorrected × 100]. Station names are shown on the vertical axis and lead time in days on the horizontal axis.

Discussion

There are several caveats and limitations to the approach described here before it could be used in an operational agricultural application. First, we obtained observed weather data from agricultural weather stations that are representative of well-watered conditions found throughout irrigated western US farms. However, most farms do not have reliable weather stations to use for bias correction of forecasts. Although a potential solution is to use the bias-correction ratios based on the nearest weather station, many farms will still be tens or hundreds of kilometers away from these stations. A second option could be to use historical ET_0 estimates from high-resolution gridded climate data (e.g., Abatzoglou 2011) that are bias-corrected to nearby agricultural weather stations to create farm-specific or even field-specific bias ratios.

A limitation of NDFD and FRET is that forecasts are deterministic and provide no level of uncertainty or confidence. Although some users may prefer to see a single forecast value, there is strong support showing ensemble forecasts are more skillful than deterministic forecasts, especially at longer lead times (e.g., Zhu 2005; Gneiting and Raftery 2005; Boucher et al. 2011). Ensemble forecast systems are costly to run and time-consuming compared with a single deterministic run, which is one reason they are rarely run at high resolution over large domains. In the case of NDFD, its high spatial resolution and short lead times (1–5 days, where

deterministic forecasts are comparable to ensemble means) used for irrigation scheduling might be sufficient. Future studies should compare ensemble and deterministic ET_0 forecasts for agricultural applications.

Intuitively, improving irrigation efficiency by using ET_0 forecasts would also lead to less water loss in the form of *ET*. Paradoxically, improving irrigation efficiencies often causes an increase in *ET*, even though the amount of applied water decreases (Grafton et al. 2018; Ward and Pulido-Velazquez 2008). Understanding this irrigation-efficiency paradox requires a detailed look at the relationships among crop *ET*, irrigation uniformity, avoidable and unavoidable consumptive uses, and beneficial and nonbeneficial consumptive uses. Burt et al. (1997) examined these relationships and identified avoidable nonbeneficial consumptive uses, including bare-soil evaporation, sprinkler wind drift, and canopy-interception losses. These losses could be reduced with conversion to LEPA techniques (Lyle and Bordovsky 1981; Bordovsky 2019). However, converting to LEPA requires significant investment ($5,000–$20,000 per center pivot), and although the Nevada Department of Agriculture recently began a drought and water conservation grant program per recommendations by the Nevada Drought Forum (Drozdoff et al. 2015), conversion has been slow across the state, and it may take decades before it is the primary irrigation method from groundwater.

From the perspective of agricultural producers, ET_0 forecasts can be used for irrigation scheduling (e.g., Wang and Cai 2009; Anupoju et al. 2021; Hamouda et al. 2022). During periods of high ET_0, water limited pivots (typically due to low well yield) can run nearly 24 h a day, 7 days a week to provide the crop with sufficient water. Knowledge of the coming week's ET_0 is useful information to help growers to apply the amount of water necessary to meet atmospheric demand but at the most efficient times of day. The grower will have confidence that enough water is provided for the coming week to satisfy the atmospheric demand while choosing the best times to irrigate such as at night or when wind speed is low.

Summary and Conclusions

This study provided an evaluation of ET_0 forecasts derived from NDFD inputs and the FRET product compared with observations

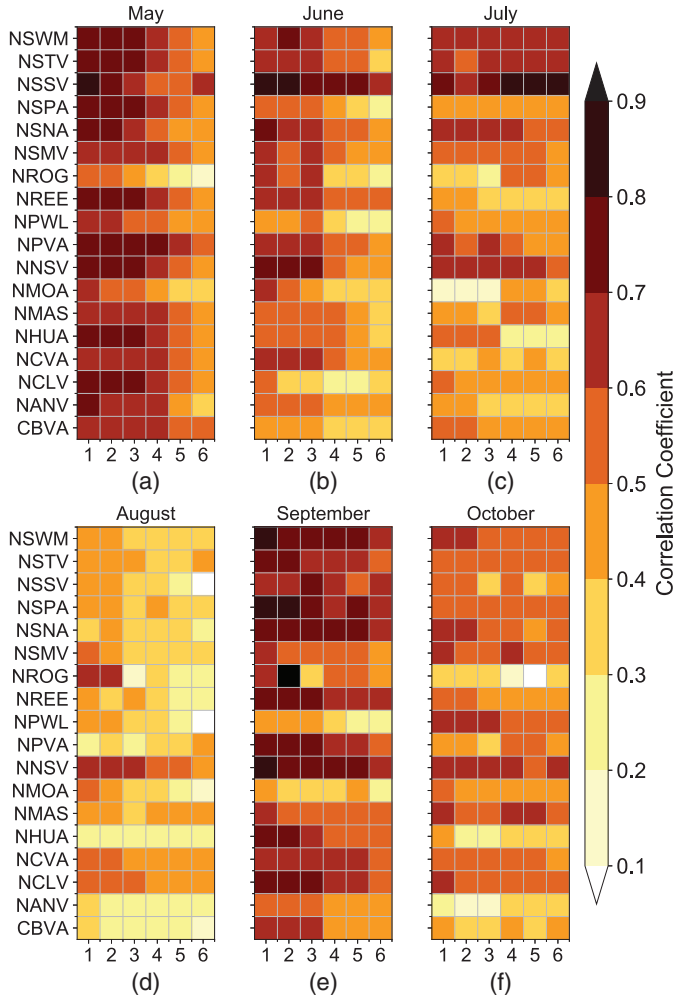

Fig. 10. (Color) Correlation coefficient R between FRET and NICE Net ET_0 in (a) May; (b) June; (c) July; (d) August; (e) September; and (f) October. Vertical axes show the station abbreviations, and horizontal axis shows lead time in days. The analysis from Fig. 3 was repeated with FRET instead of NDFD ET_0 to create this figure.

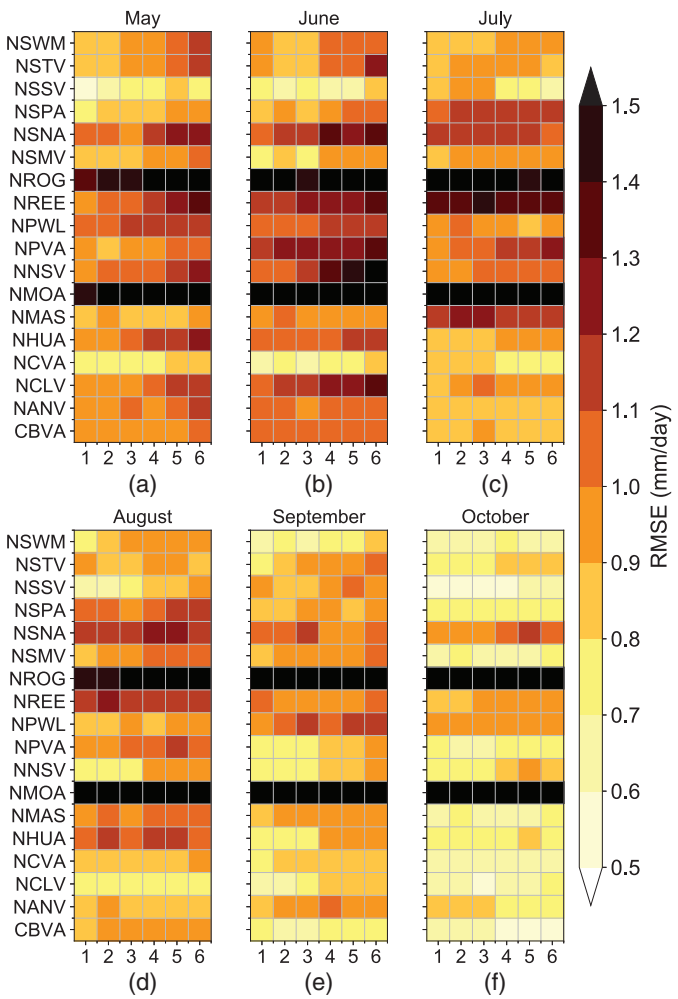

Fig. 11. (Color) RMSE between FRET and NICE Net ET_0 in (a) May; (b) June; (c) July; (d) August; (e) September; and (f) October. Vertical axes show the station abbreviations, and horizontal axis shows lead time in days. The analysis from Fig. 5 was repeated with FRET instead of NDFD ET_0 to create this figure.

from the NICE Net. We also demonstrated the value of implementing a bias-correction method to improve RMSE. We showed results from NDFD in the main paper (with FRET given in Appendix I) because NDFD allowed for a longer period of record as well as analysis of the individual drivers of ET_0, which ultimately control resultant ET_0 quantities.

ET_0 forecasts were reasonably well correlated to observations during most of the growing season, with notable declines in correlations during July and August, and generally decreasing correlations with lead time. Systematic biases were found in T_{max}, T_{min}, vapor pressure, and solar radiation from NDFD. An arid bias that arises due to NDFD not accounting for irrigated lands and the associated modified near-surface boundary layer was apparent in NDFD T_{min}, which is biased high year-round (often exceeding +3°C in summer), and during the growing season T_{max} typically biased high and vapor pressure biased low.

A case study revealed that observed daily variability in T_{min}, solar radiation, wind speed, and ET_0 was underestimated by NDFD and is likely a key factor in reducing the skill of the forecast ET_0 (also supported by the skill analysis of each driver). Solar radiation on cloudy days showed minimal decreases in NDFD compared with observations, which has a cascading effect impacting all other variables and the estimated ET_0. Other studies have documented this observed effect of how clouds have a strong influence on diurnal temperature ranges (Dai et al. 1999; Zhou et al. 2009; Tang and Leng 2013). The poor representation of convective clouds in NDFD could be a result of the model physics not capturing the physical processes, the crude estimate of solar radiation from percent sky cover, a grid scale/point scale mismatch, or a combination of all of these.

Application of bias-correction ratios to ET_0 generally reduced RMSE daily values by 5%–30%. Testing other bias-correction methods (e.g., Durai and Bhradwaj 2014) or correcting the ET_0 input variables first (e.g., Yang et al. 2021) is recommended in future studies to determine if other methods may provide better forecast skill than the ratio method used in this study. It is yet to be seen whether the level of skill from these bias-corrected forecasts is sufficient to aid farmers in irrigation scheduling and water-conservation efforts. Future efforts will focus on engagement with producers to better understand data needs, desired forecast skill for reliable irrigation scheduling, and data-delivery systems (i.e., web applications).

Appendix I. FRET Compared with Observations

This appendix is intended to show that results obtained using FRET are comparable to those from ET_0 we computed from individual

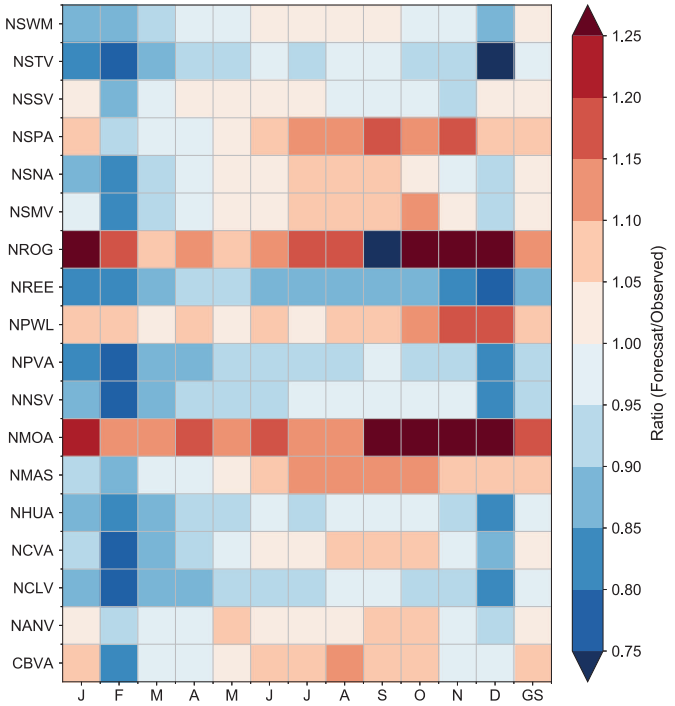

Fig. 12. (Color) FRET bias ratios for the lead 1-day forecasts. Horizontal axes show the calendar months (January–December) from left to right with the growing season (May–October) average on the far right. Vertical axes show the station abbreviations. Analysis from Fig. 7(d) was repeated with FRET instead of NDFD ET_0 to create this figure.

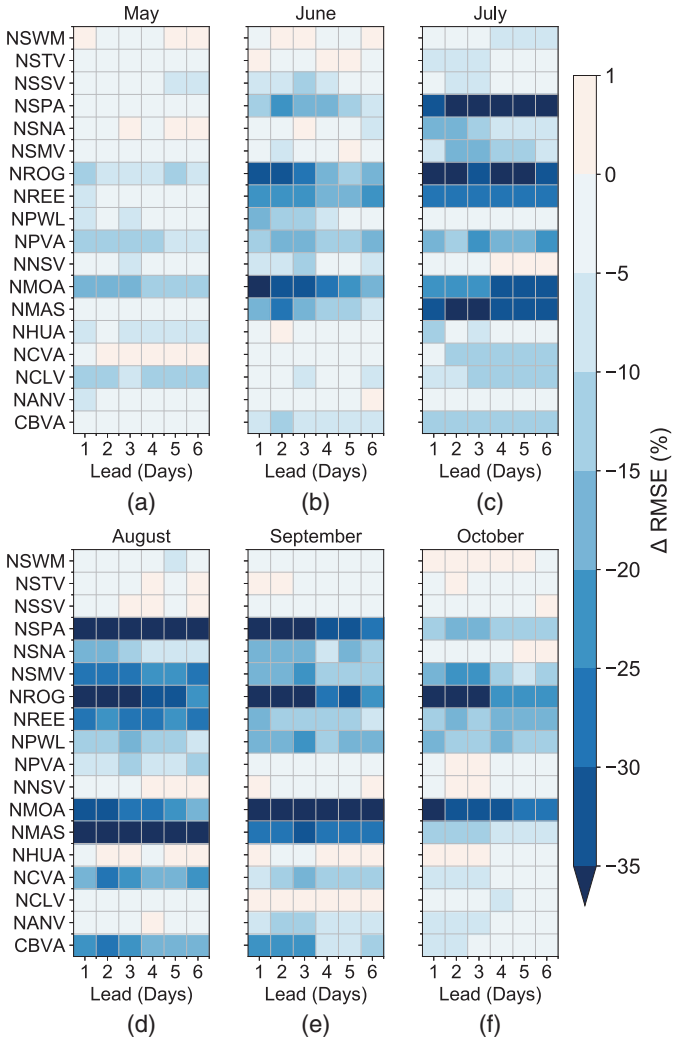

Fig. 13. (Color) Percent change in FRET RMSE at all lead times for (a) May; (b) June; (c) July; (d) August; (e) September; and (f) October. Percent change is calculated as [(bias corrected − uncorrected)/uncorrected × 100]. Station names are shown on the vertical axis, and lead time in days on the horizontal axis. Analysis from Fig. 9 was repeated with FRET instead of NDFD ET_0 to create this figure.

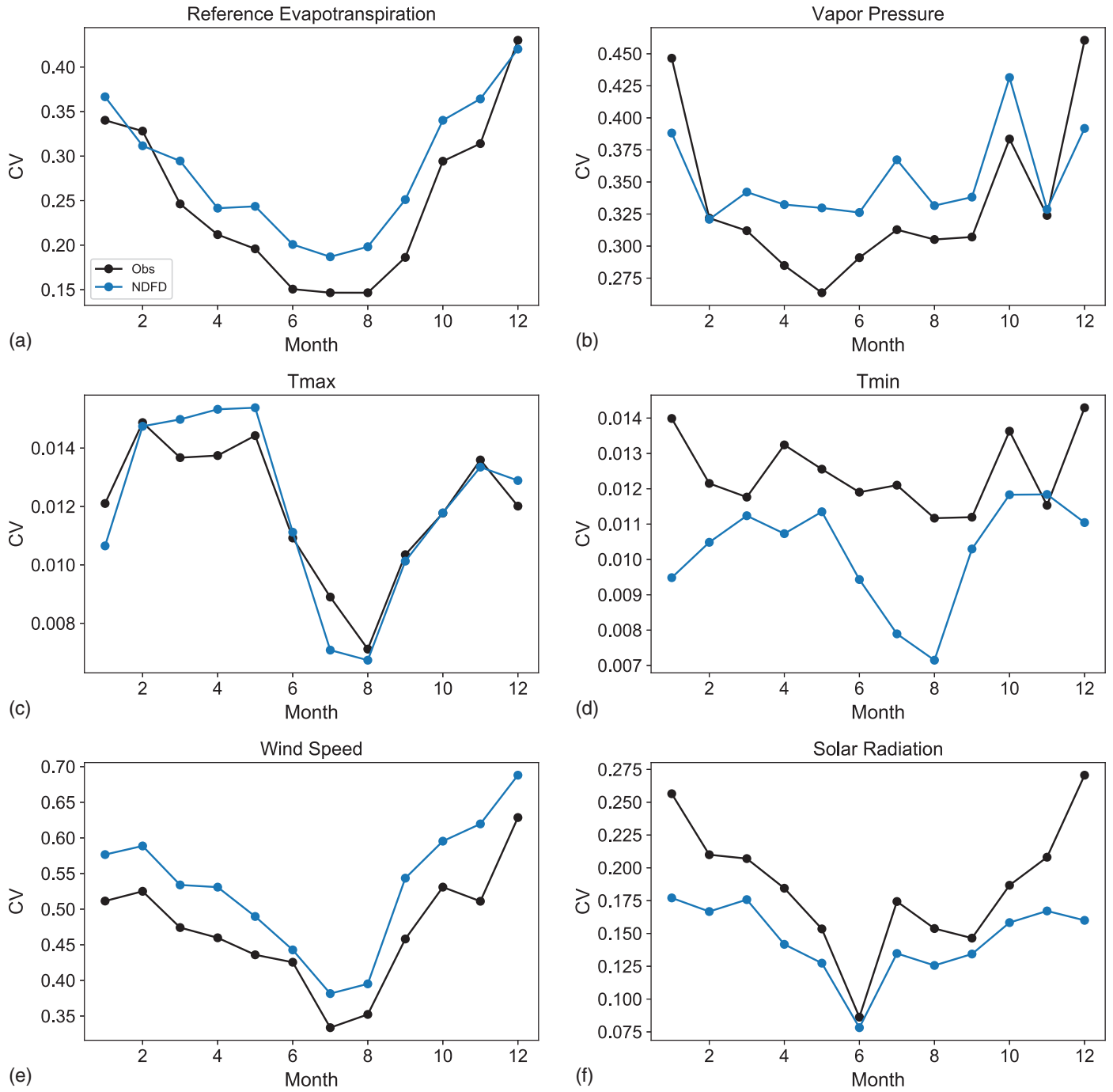

Fig. 14. (Color) Daily time series for July 2018 at NMOA (Obs) and nearest NDFD grid point for (a) ET_0; (b) vapor pressure; (c) T_{max}; (d) T_{min}; (e) wind speed; and (f) solar radiation. NDFD forecasts shown are for a 1-day lead time.

NDFD drivers (Figs. 10–13). In an operational setting, FRET will likely be used. The "Data and Methods" section provides more details on the differences between FRET and our NDFD ET_0 data sets and why NDFD ET_0 was used in the main sections of the study.

Appendix II. Moapa Valley Case Study

Two figures are shown here to complement Figs. 7 and 8. These figures show Moapa Valley (NMOA),which is one of the sites with the worst forecast skill. Compared with Figs. 7 and 8, NMOA shows some similarities and some differences. The main similarities are that both sites showed NDFD underestimates the T_{min} and solar radiation variability. However, NMOA showed NDFD overestimates the ET_0 and wind speed variability (Fig. 14) which is opposite of the NSMV results. The time series for NMOA (Fig. 15) shows that the ET_0 variations tracked wind speed variations quite closely, which makes sense because wind is the dominant driver of ET_0 variability in southern Nevada during the growing season (Hobbins 2016). Fig. 6 showed very large positive wind speed biases at NMOA, which could be one of the main reasons the overall skill is so poor for this site.

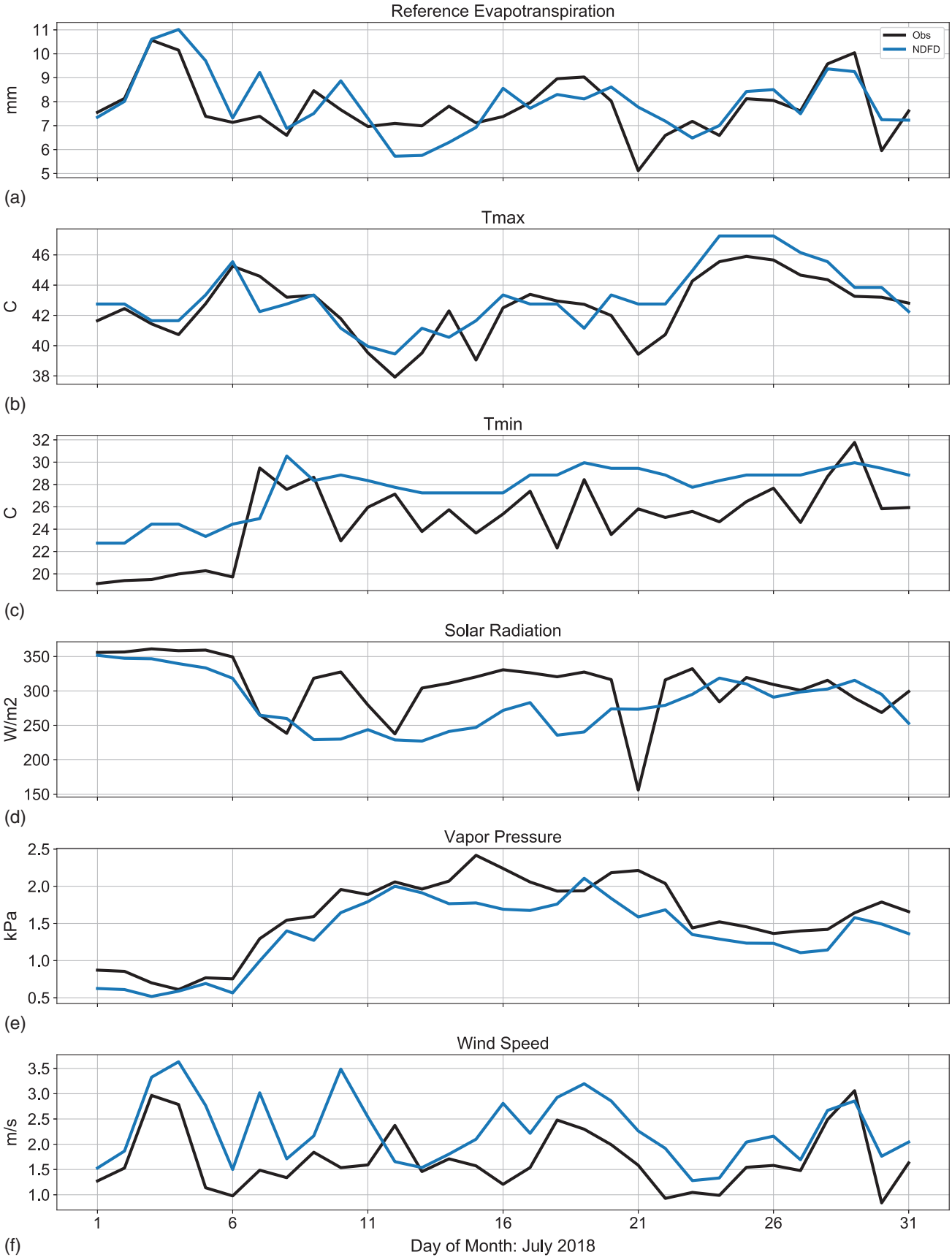

Fig. 15. (Color) Monthly (daily values averaged to the month) COV at the Moapa Valley NICE Net (NMOA) (marked Obs) and nearest NDFD grid point for (a) ET_0; (b) vapor pressure; (c) T_{max}; (d) T_{min}; (e) wind speed; and (f) solar radiation. NDFD forecasts shown are for a 1-day lead time.

Data Availability Statement

The pyWeatherQAQC code used to QC observations can be found at https://github.com/WSWUP/pyWeatherQAQC. Code use to compute the ASCE Standardized Reference *ET* for observations and data can be found at https://github.com/WSWUP/RefET. Weather station data from NICE Net were provided by the Desert Research Institute and can be found at https://nicenet.dri.edu/. Forecast data from NDFD were provided by NOAA's National Center for Environmental Information and can be found at https://www.ncdc.noaa.gov/data-access/model-data/model-datasets/national-digital-forecast-database-ndfd.

Acknowledgments

This work was funded by the Nevada National Science Foundation's Experimental Program to Stimulate Competitive Research (NSF EPSCoR) Undergraduate Research Opportunity Program (UROP) and by NOAA's National Integrated Drought Information System California-Nevada Drought Early Warning System under Award No. NA20OAR4310253C.

References

Abatzoglou, J. T. 2011. "Development of gridded surface meteorological data for ecological applications and modeling." *Int. J. Climatol.* 33 (1): 121–131. https://doi.org/10.1002/joc.3413.

Allen, R. 2008. "Quality assessment of weather data and micrometeological flux-impacts on evapotranspiration calculation." In *Proc., Annual Meeting of the Society of Agricultural Meteorology of Japan Abstracts of Int. Symposium on Agricultural Meteorology 2008*, 25–41. Tokyo: Society of Agricultural Meteorology of Japan.

Allen, R., et al. 2015. "Evapotranspiration mapping for water security: Recommendations and requirements." In *Proc., Recommendations from the Participants of the 2015 Workshop on Evapotranspiration Mapping for Water Security.* Washington, DC: NASA Applied Sciences Program Water Resources Program and the World Bank.

Allen, R. G. 1996. "Assessing integrity of weather data for reference evapotranspiration estimation." *J. Irrig. Drain. Eng.* 122 (2): 97–106. https://doi.org/10.1061/(ASCE)0733-9437(1996)122:2(97).

Allen, R. G., C. E. Brockway, and J. L. Wright. 1983. "Weather station siting and consumptive use estimates." *J. Water Resour. Plann. Manage.* 109 (2): 134–136. https://doi.org/10.1061/(ASCE)0733-9496(1983)109:2(134).

Allen, R. G., L. S. Pereira, T. A. Howell, and M. E. Jensen. 2011. "Evapotranspiration information reporting: I. Factors governing measurement accuracy." *Agric. Water Manage.* 98 (6): 899–920. https://doi.org/10.1016/j.agwat.2010.12.015.

Allen, R. G., I. A. Walter, R. Elliott, T. A. Howell, D. Itenfisu, and M. E. Jensens. 2005. *The ASCE standardized reference evapotranspiration equation*. Reston, VA: ASCE.

Allmaras, R. R., D. E. Wilkins, O. C. Burnside, and D. J. Mulla. 2018. "Agricultural technology and adoption of conservation practices." In *Advances in soil and water conservation*, edited by F. J. Pierce and W. W. Frye, 99–158. Chelsea, MI: Ann Arbor Press. https://doi.org/10.1201/9781315136912.

Anupoju, V., B. P. Kambhammettu, and S. K. Regonda. 2021. "Role of short-term weather forecast horizon in irrigation scheduling and crop water productivity of rice." *J. Water Resour. Plann. Manage.* 147 (8): 05021009. https://doi.org/10.1061/(ASCE)WR.1943-5452.0001406.

Blankenau, P. 2017. "Bias and other error in gridded weather data sets and their impacts on estimating reference evapotranspiration." M.S. thesis, Dept. of Civil and Environmental Engineering, Univ. of Nebraska-Lincoln.

Blumler, M. A. 2018. "The West without water: What past floods, droughts, and other climatic clues tell us about tomorrow." In *The AAG review of books*, 15–17. Berkley, CA: University of California Press. https://doi.org/10.1080/2325548X.2018.1402269.

Bordovsky, J. P. 2019. "Low-energy precision application (LEPA) irrigation: A forty-year review." *Trans. ASABE* 62 (5): 1343–1353. https://doi.org/10.13031/trans.13117.

Boucher, M. A., F. Anctil, L. Perreault, and D. Tremblay. 2011. "A comparison between ensemble and deterministic hydrological forecasts in an operational context." *Adv. Geosci.* 29 (Mar): 85–94. https://doi.org/10.5194/adgeo-29-85-2011.

Brutsaert, W. 2013. *Vol. 1 of Evaporation into the atmosphere: Theory, history and applications*. New York: Springer.

Brutsaert, W., and M. B. Parlange. 1998. "Hydrologic cycle explains the evaporation paradox." *Nature* 396 (5): 300. https://doi.org/10.1038/23845.

Burt, C. M., A. J. Clemmens, T. S. Strelkoff, K. H. Solomon, R. D. Bliesner, L. A. Hardy, T. A. Howell, and D. E. Eisenhauer. 1997. "Irrigation performance measures: Efficiency and uniformity." *J. Irrig. Drain. Eng.* 123 (6): 423–442. https://doi.org/10.1061/(ASCE)0733-9437(1997)123:6(423).

Dai, A., K. E. Trenberth, and T. R. Karl. 1999. "Effects of clouds, soil moisture, precipitation, and water vapor on diurnal temperature range." *J. Clim.* 12 (8): 2451–2473. https://doi.org/10.1175/1520-0442(1999)012<2451:EOCSMP>2.0.CO;2.

Daly, C., W. P. Gibson, G. H. Taylor, G. L. Johnson, and P. Pasteris. 2002. "A knowledge-based approach to the statistical mapping of climate." *Clim. Res.* 22 (2): 99–113. https://doi.org/10.3354/cr022099.

Desert Research Institute. n.d.-a. "Nevada integrated climate and evapotranspiration network." Accessed May 1, 2020. https://nicenet.dri.edu/.

Desert Research Institute. n.d.-b. "Western states water use program: pyWeatherQAQC." Accessed May 13, 2020. https://github.com/WSWUP/pyWeatherQAQC.

Dieter, C. A., M. A. Maupin, R. R. Caldwell, M. A. Harris, T. I. Ivahnenko, J. K. Lovelace, and K. S. Linsey. 2018. *Estimated use of water in the United States in 2015, US Geological Survey, circular 1441.* Washington, DC: USGS. https://doi.org/10.3133/cir1441.

Drozdoff, L., J. Ensminger, J. Barbee, D. Boyle, M. Walker, J. Huntington, and C. Cage. 2015. "Nevada drought forum: Recommendations report presented to Governor Brian Sandoval." Accessed January 15, 2021. http://www.dri.edu/images/stories/divisions/dhs/dhsfaculty/Justin-Huntington/Executive_Summary_ASTP.pdf.

Durai, V. R., and R. Bhradwaj. 2014. "Evaluation of statistical bias correction methods for numerical weather prediction model forecasts of maximum and minimum temperatures." *Nat. Hazard.* 73 (3): 1229–1254. https://doi.org/10.1007/s11069-014-1136-1.

Engle, S., D. DuBois, and J. Shoemake. 2019. "A shootout between forecast reference evapotranspiration (FRET) and ZiaMet weather station data for calculating reference ET." In *Proc., 33rd Conf. on Hydrology.* Phoenix: American Meteor Society.

Fipps, G., and L. L. New. 1990. "Six years of LEPA in Texas—Less water, higher yields. Visions of the future." In *Proc., 3rd National Irrigation Symp.*, 115–120. St. Joseph, MI: American Society for Agricultural Engineers.

Glahn, H. R., and D. P. Ruth. 2003. "The new digital forecast database of the national weather service." *Bull. Am. Meteorol. Soc.* 84 (2): 195–202. https://doi.org/10.1175/BAMS-84-2-195.

Gneiting, T., and A. E. Raftery. 2005. "Weather forecasting with ensemble methods." *Science* 310 (5746): 248–249. https://doi.org/10.1126/science.1115255.

Grafton, R. Q., et al. 2018. "The paradox of irrigation efficiency." *Science* 361 (6404): 748–750. https://doi.org/10.1126/science.aat9314.

Hamouda, B., D. Zaccaria, K. Bali, R. L. Snyder, and F. Ventura. 2022. "Evaluation of forecast reference evapotranspiration for different microclimate regions in California to enable prospective irrigation scheduling." *J. Irrig. Drain. Eng.* 148 (1): 04021061. https://doi.org/10.1061/(ASCE)IR.1943-4774.0001632.

Hobbins, M. T. 2010. "What are evapotranspiration and forecast reference crop evapotranspiration (FRET)?" Accessed January 15, 2021. https://www.wrh.noaa.gov/forecast/evap/FRET/ExplainingFRETscientific.pdf.

Hobbins, M. T. 2016. "The variability of ASCE standardized reference evapotranspiration: A rigorous, CONUS-Wide decomposition and attribution." *Trans. ASABE* 59 (2): 561–576. https://doi.org/10.13031/trans.59.10975.

Hobbins, M. T., and J. L. Huntington. 2016. "Evapotranspiration and evaporative demand." Chap. 42 in *Handbook of applied hydrology*, edited by V. P. Singh. New York: McGraw-Hill Education.

Hobbins, M. T., J. A. Ramírez, and T. C. Brown. 2004. "Trends in pan evaporation and actual evaporation across the conterminous US: Paradoxical or complementary?" *Geophys. Res. Lett.* 31 (13): L13503. https://doi.org/10.1029/2004GL019846.

Huntington, J. L., M. Bromley, C. Morton, and T. Minor. 2018. *Remote sensing estimates of evapotranspiration from irrigated agriculture, Northwestern Nevada and Northeastern California*. Desert Research Institute Rep. No. 41275. Reno, NV: Desert Research Institute.

Huntington, J. L., S. Gangopadhyay, M. Spears, R. Allen, D. King, C. Morton, A. Harrison, D. McEvoy, and A. Joros. 2015. *West-wide climate risk assessments: Irrigation demand and reservoir evaporation projections*. US Bureau of Reclamation Technical Memorandum No. 68-68210-2014-01. Denver: US Department of the Interior Bureau of Reclamation Technical Service Center.

Huntington, J. L., C. Morton, D. McEvoy, M. Bromley, K. Hedgewisch, R. Allen, and S. Gangopadhyay. 2016. *Historical and future irrigation water requirements for selected reclamation project areas.* Western US Desert Research Institute Report. Reno, NV: Desert Research Institute.

Krone-Davis, P., F. S. Melton, H. D. Snell, C. Palmer, and C. Rosevelt. 2012. "Comparison of NOAA experimental forecasted reference evapotranspiration and observed CIMIS reference evapotranspiration." In *Proc., American Geophysical Union 2012 Fall Conf.* Washington, DC: American Geophysical Union.

Lewis, C. S., H. M. Geli, and C. M. Neale. 2014. "Comparison of the NLDAS weather forcing model to agrometeorological measurements in the western United States." *J. Hydrol.* 510 (Mar): 385–392. https://doi.org/10.1016/j.jhydrol.2013.12.040.

Lyle, W. M., and J. P. Bordovsky. 1981. "Low energy precision application (LEPA) irrigation system." *Trans. ASAE* 24 (5): 1241–1245. https://doi.org/10.13031/2013.34427.

Lyle, W. M., and J. P. Bordovsky. 1983. "LEPA irrigation system evaluation." *Trans. ASAE.* 26 (3): 776–781. https://doi.org/10.13031/2013.34022.

Mitchell, K. E., et al. 2004. "The multi-institution North American land data assimilation system (NLDAS): Utilizing multiple GCIP products and partners in a continental distributed hydrological modeling system." *J. Geophys. Res.* 109 (Apr): D07S90. https://doi.org/10.1029/2003JD003823.

NASS (National Agriculture Statistics Service). 2019. "Census of agriculture: United States summary and state data. Volume 1. Geographic area series. Part 51." Accessed January 15, 2021. https://www.nass.usda.gov/Publications/AgCensus/2017/Full_Report/Volume_1,_Chapter_1_US/usv1.pdf.

NWS (National Weather Service). 2018. "National digital forecast database definitions. NOAA's national weather service." Accessed October 26, 2018. https://www.digital.weather.gov/staticpages/definitions.php.

Ozdogan, M., and M. Rodell. 2010. "Simulating the effects of irrigation over the united states in a land surface model based on satellite-derived agricultural data." *J. Hydrometeorol.* 11 (1): 171–184. https://doi.org/10.1175/2009JHM1116.1.

Rajan, N., S. Maas, R. Kellison, M. Dollar, S. Cui, S. Sharma, and A. Attia. 2015. "Emitter uniformity and application efficiency for centre-pivot irrigation systems." *Irrig. Drain.* 64 (3): 353–361. https://doi.org/10.1002/ird.1878.

Szilagyi, J., and A. Schepers. 2014. "Coupled heat and vapor transport: The thermostat effect of a freely evaporating land surface." *Geophys. Res. Lett.* 41 (2): 435–441. https://doi.org/10.1002/2013GL058979.

Tang, Q., and G. Leng. 2013. "Changes in cloud cover, precipitation, and summer temperature in North America from 1982 to 2009." *J. Clim.* 26 (5): 1733–1744. https://doi.org/10.1175/JCLI-D-12-00225.1.

Temesgen, B., R. G. Allen, and D. T. Jensen. 1999. "Adjusting temperature parameters to reflect well-watered conditions." *J. Irrig. Drain. Eng.* 125 (1): 26–33. https://doi.org/10.1061/(ASCE)0733-9437(1999)125:1(26).

Tian, D., and C. J. Martinez. 2014. "The GEFS-based daily reference evapotranspiration (*ET*o) forecast and its implication for water management in the southeastern United States." *J. Hydrometeorol.* 15 (3): 1152–1165. https://doi.org/10.1175/JHM-D-13-0119.1.

Walter, I. A., et al. 2000. "ASCE's standardized reference evapotranspiration equation." In *Watershed management and operations management 2000*, 1–11. Reston, VA: ASCE. https://doi.org/10.1061/40499(2000)126.

Wang, D., and X. Cai. 2009. "Irrigation scheduling—Role of weather forecasting and farmers' behavior." *J. Water Resour. Plann. Manage.* 135 (5): 364–372. https://doi.org/10.1061/(ASCE)0733-9496(2009)135:5(364).

Ward, F. A., and M. Pulido-Velazquez. 2008. "Water conservation in irrigation can increase water use." *Proc. Natl. Acad. Sci. USA* 105 (47): 18215–18220. https://doi.org/10.1073/pnas.0805554105.

Yang, Q., Q. J. Wang, K. Hakala, and Y. Tang. 2021. "Bias-correcting input variables enhances forecasting of reference crop evapotranspiration." *Hydrol. Earth Syst. Sci.* 25 (9): 4773–4788. https://doi.org/10.5194/hess-25-4773-2021.

Zhou, L., A. Dai, Y. Dai, R. S. Vose, C. Z. Zou, Y. Tian, and H. Chen. 2009. "Spatial dependence of diurnal temperature range trends on precipitation from 1950 to 2004." *Clim. Dyn.* 32 (2): 429–440. https://doi.org/10.1007/s00382-008-0387-5.

Zhu, Y. 2005. "Ensemble forecast: A new approach to uncertainty and predictability." *Adv. Atmos. Sci.* 22 (6): 781–788. https://doi.org/10.1007/BF02918678.